

## Supplementary Information for

Genetic Deletion of Vesicular Glutamate Transporter in Dopamine Neurons Increases  
Vulnerability to MPTP-Induced Neurotoxicity in Mice

Hui Shen<sup>1</sup>, Rosa Anna M. Marino<sup>1</sup>, Ross A. McDevitt<sup>1</sup>, Guo-Hua Bi<sup>1</sup>, Kai Chen<sup>1</sup>, Graziella  
Madeo<sup>1</sup>, Pin-Tse Lee<sup>1</sup>, Ying Liang<sup>1</sup>, Lindsay M. De Biase<sup>1</sup>, Tsung-Ping Su<sup>1</sup>, Zheng-Xiong  
Xi<sup>1</sup>, Antonello Bonci<sup>1,2,3,4,5\*</sup>

\*Corresponding: Antonello Bonci

[antonello.bonci@nih.gov](mailto:antonello.bonci@nih.gov)

### **This PDF file includes:**

Supplementary text  
Figs. S1 to S8  
References for SI reference citations

## Supplementary Information Text

### Experimental Procedures

#### Animals

Conditional VgluT2-knockout (cKO) mice were bred at the National Institute on Drug Abuse (NIDA), Intramural Research Program (IRP). DAT-*VgluT2*<sup>-/-</sup> mice were generated by crossing DAT-Cre (heterozygous) transgenic mice (129/Sv/J background, Jackson Laboratories) with *VgluT2*<sup>flx/flx</sup> mice (129, C57 Bl/6 background, Jackson Laboratories) carrying the exon 2 surrounded by loxP sites. A breeding colony was maintained by mating DAT-Cre mice with *VgluT2*<sup>flx/flx</sup> mice. Twenty-five percent of the offspring from such mating were thus used as controls (i.e., DAT-Cre;*VgluT2*<sup>flx/-</sup>, i.e., VgluT2-Het mice) and 25% lacked *VgluT2* in DA neurons (i.e., DAT-Cre;*VgluT2*<sup>flx/flx</sup>, i.e., VgluT2-cKO mice). Only male littermates of such mating were used as study subjects. The mutant lines were bred for >10 generations on the background of C57BL/6 mice from Charles River Laboratories (Frederick, MD, USA).

#### Intracranial microinjection surgeries

Male mice were anesthetized with sodium pentobarbital (60 mg/kg, i.p.) and placed in a stereotaxic frame (David Kopf Instruments, Tujunga, CA, USA). For intra-VTA microinjection of virus, a custom-made 30-gauge stainless injector was used to infuse Cre-inducible AAV bilaterally into the VTA (AP -3.42; ML 1.62; DV -4.92 mm relative to Bregma) using a micropump (WPI 2000 UltraMicroPump, Sarasota, FL, USA). The three viral vectors were AAV5-EF1 $\alpha$ -DIO-ChR2-EYFP (provided by University of North Carolina Gene Therapy Center) that encodes channelrhodopsin-2 (ChR2) and enhanced green fluorescent protein (GFP) (for

electrophysiological studies), AAV5-EF1a-DIO-VgluT2-T2A-GFP (provided by ViGene Biosciences, Inc.) that encodes VgluT2 and enhanced green GFP (for VgluT2 overexpression experiments), or AAV5-EF1a-DIO-T2A-GFP (provided by ViGene Biosciences, Inc.) that encodes enhanced GFP only (control group). The AAV injection amount was ~600 nl containing  $\sim 2 \times 10^{13}$  genomes/ml AAV-ChR2, AAV-VgluT2, or AAV-GFP viruses and the speed was 50 nl/min. The VgluT2 overexpression-related experiments began 4 weeks after the AAV vector injections, and the electrophysiological experiments began 8 weeks after the AAV vector injections.

### **Behavioral tests**

Behavioral tests were carried out from day 14 after MPTP (Sigma-Aldrich, 18 mg/kg  $\times$  4, with 2 hrs inter-injection intervals) or saline injections in mice without intracranial AAV injections, or in mice 4 weeks after intracranial AAV-VgluT2 microinjections. The following tests were performed to evaluate the effects of MPTP on motor deficits.

### **Open-field locomotion**

This experiment was designed to study the effects of MPTP on open-field locomotor behavior between the VgluT2-cKO mice (or VgluT2-rescued) and their Het littermate control mice.

Animals were placed in the locomotor chambers for 2 hours, 14 days after MPTP treatment. The travel distance, horizontal, and vertical activity counts were used to evaluate the effects of MPTP on locomotion.

### **Rotarod test**

Rotarod test was conducted to evaluate the motor coordination ability of the mice after MPTP or

saline administration. The apparatus had a four-lane rotating rod (1.25 inch in diameter) (AccuScan Instruments Inc., Columbus, Ohio, USA). The speed of rotation of the rotarod was increased from 4 to 40 rpm over 2 min. After 2–3 days of habituation and training on the rotarod device (3 times per day), animals were placed on the rotarod device to observe their locomotor performance on the test day. Once the mouse fell off the rod, the recorder was stopped. Each mouse was subjected to three trials, at 10 min intervals, with a maximum of 5 min per trial. The average time (sec) that each mouse held on to the rotating rod during three trials was used to evaluate motor coordination ability after MPTP or saline treatment.

### **Parallel rod floor test**

Parallel floor rod test is a tool for assessing locomotor function in rodent models of CNS disorders. Subjects were placed on an elevated horizontal ladder and trained to cross the device. This test evaluated the ability of the mice to accurately place the front paws or hind paws during spontaneous exploration of an elevated grid or ladder (1). In brief, mice were placed on a  $21 \times 21.5 \text{ cm}^2$  wire grid (iron wires at 1.6 mm in diameter) (Accusan, Columbia, OH, USA). Mice were allowed to freely move for 300 sec. A computer recorded paws slipping along the steps of the ladder as the animal crossed. Paw misplacements and the ambulatory time were recorded for each run of the test; a total of four runs are recorded for each animal. The mice were put on the grid twice for habituation before the test. Each test was repeated three times (trials). The average of foot slips/misplacements in each trial was used to evaluate the locomotor performance on parallel rods.

### **Elevated plus maze**

The elevated plus maze apparatus (Med Associates, Inc) was placed 30 cm above the floor and

consisted of two plastic light gray open arms (30 × 5 cm) and two black closed arms (30 × 5 cm) extending from a central platform (5 × 5 × 5 cm) at 90 degrees. Mice were individually placed in the center. Video tracking Ethovision software (Noldus Information Technology) was used to track mouse location, and total time spent in the open and closed arms. All experiment sessions lasted 5 minutes. The maze was cleaned with 70% ethanol after every trial and allowed to dry before the next series of experiments.

### **Electrophysiology**

VgluT2-Het and VgluT2-cKO mice were bilaterally injected with 0.5 µl of AAV5-DIO-ChR2-EYFP (and VVA5-DIO-VgluT2-EYFP in the VgluT2-rescued experiments) viral vector into the VTA. Electrophysiological recordings began 8-10 weeks after the viral vector injections as described (2). Briefly, animals were anesthetized and perfused with ice-cold artificial cerebrospinal fluid (ACSF). Brains were cut into 200 µm coronal sections in ice-cold ACSF. Tissue was recovered for 10 min at 32°C and then held in standard ACSF for at least 60 minutes prior to recording. The ACSF used to perfuse mice, cut, and recover tissue contained N-methyl-D-glutamine (NMDG), in substitute for sodium, and contained (in mM): 92 NMDG, 20 HEPES pH 7.35, 25 glucose, 30 sodium bicarbonate, 1.2 sodium phosphate, 2.5 potassium chloride, 5 sodium ascorbate, 3sodium pyruvate, 2 thiourea, 10 magnesium sulfate, and 0.5 calcium chloride. ACSF for holding tissue prior to recordings had the following modifications: 92 mM sodium chloride in place of NMDG, 1 mM magnesium chloride, and 2 mM calcium chloride. Recordings were obtained while perfusing tissue with ACSF containing (in mM): 125 sodium chloride, 2.5 potassium chloride, 1.25 sodium phosphate, 1 magnesium chloride, 2.4 calcium chloride, 26 sodium bicarbonate, and 11 glucose. Prior to recording, expression of optogenetic protein was confirmed by visualization of EYFP fluorescence in NAc and VTA tissues. Whole-cell patch-

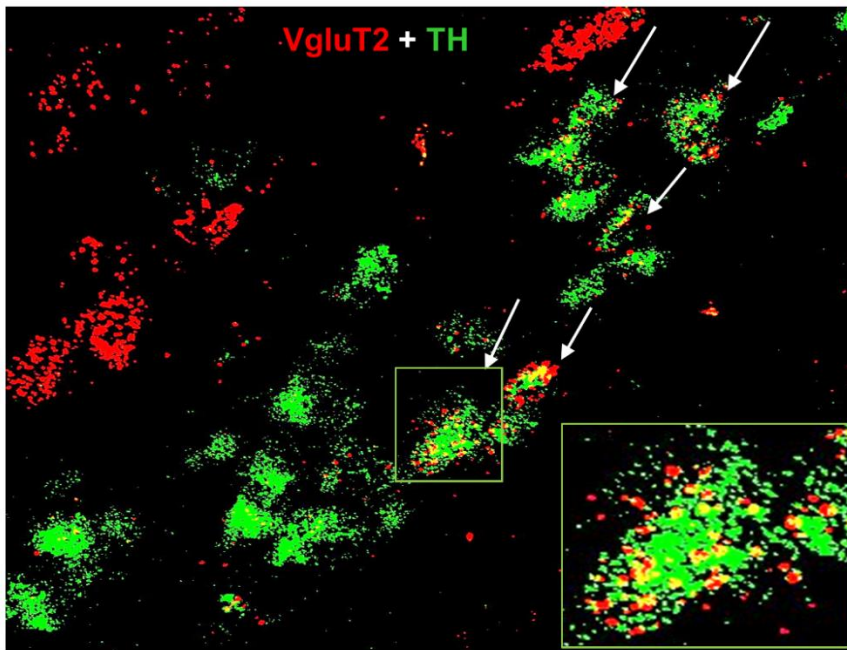
clamp recordings were performed using glass pipets with 2.4-3.2 M $\Omega$  resistance, filled with internal solution containing (in mM): 135 potassium gluconate, 10 HEPES pH 7.35, 4 potassium chloride, 4 Mg-ATP, and 0.3 Na-GTP. Recordings were performed within eYFP-expressing portions of the dorsomedial NAc shell, a projection target of glutamatergic VTA neurons (3,4). Medium spiny neurons were identified on the basis of morphological and electrophysiological properties (5). Cells were optogenetically stimulated every 30 seconds with 1 ms pulses of 10 mW, 473 nm light. A subset of neurons displaying optically-evoked excitatory post-synaptic currents (EPSCs) were pharmacologically challenged with 10  $\mu$ M DNQX.

### **Western blotting**

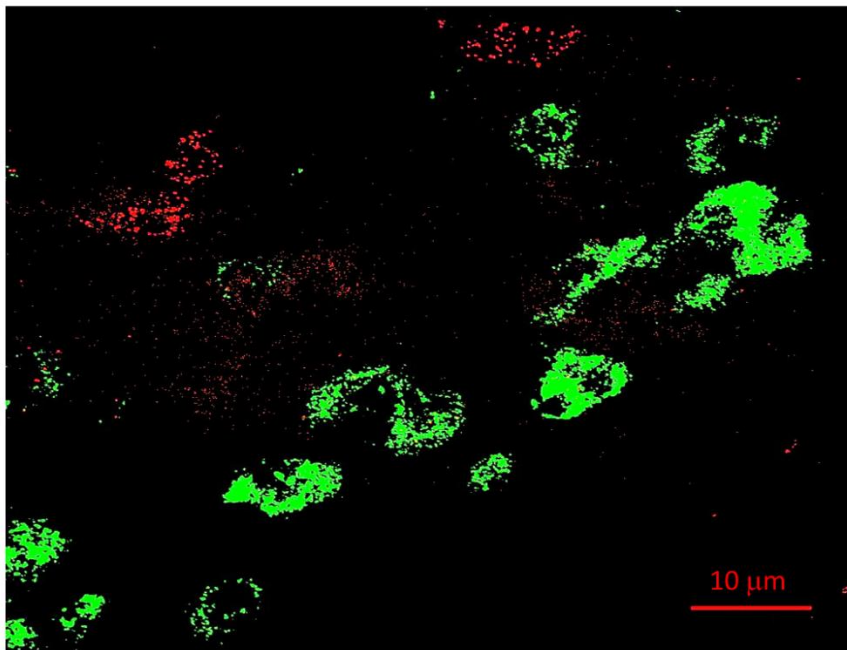
Western blot analysis was performed with the procedures, as reported previously (6, 7). Mice were perfused transcardially with cold 0.9% saline under deep anesthesia. Whole striatum and midbrain containing the VTA and SNc were dissected. Tissues were homogenized in RIPA lysis buffer (Cell Signaling Technology), and the protein concentration for each sample was quantified with a Bio-Rad Protein Assay. A total of 30  $\mu$ g of proteins was used for the immunoblot assay. Membranes were then incubated with primary antibodies [rat anti-DA transporter (DAT) monoclonal antibody (1:1,000; Millipore), rabbit anti-Bax (1:100; Millipore), goat anti-Bcl2 (1:100; Santa Cruz Biotechnology, CA), or mouse monoclonal anti- $\beta$ -actin antibody (1:2,500; Sigma-Aldrich)], and then incubated with secondary antibodies [IRDye 800CW Donkey anti-rabbit IgG for Bax, IRDye 680CW Donkey anti-goat IgG for Bcl-2, or IRDye 680CW Donkey anti-mouse for  $\beta$ -actin (LI-COR Biosciences)]. Membranes were then scanned using a LI-COR Odyssey Image System. Band density was measured using ImageJ software (<http://rsb.info.nih.gov/ij/>) (National Institutes of Health, Bethesda, MD, USA).

**Figure S1:**

**A (Het - SNc)**

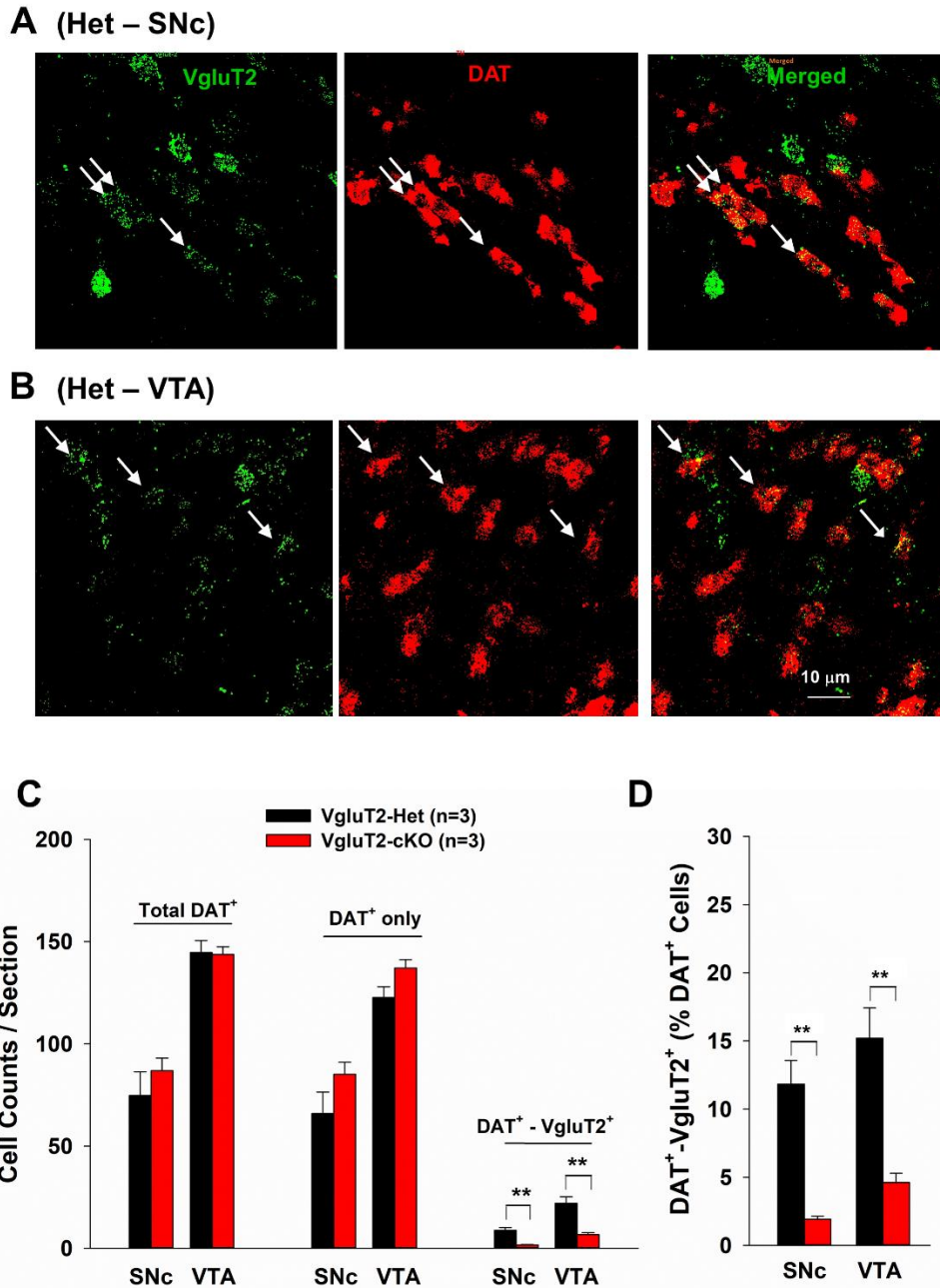


**B (cKO - SNc)**



**Figure S1**, Related to Fig. 1: Magnified images in Fig. 1C, illustrating VgluT2 and TH co-localization in a subpopulation of SNc DA neurons in Het mice, but not in VgluT2-cKO mice.

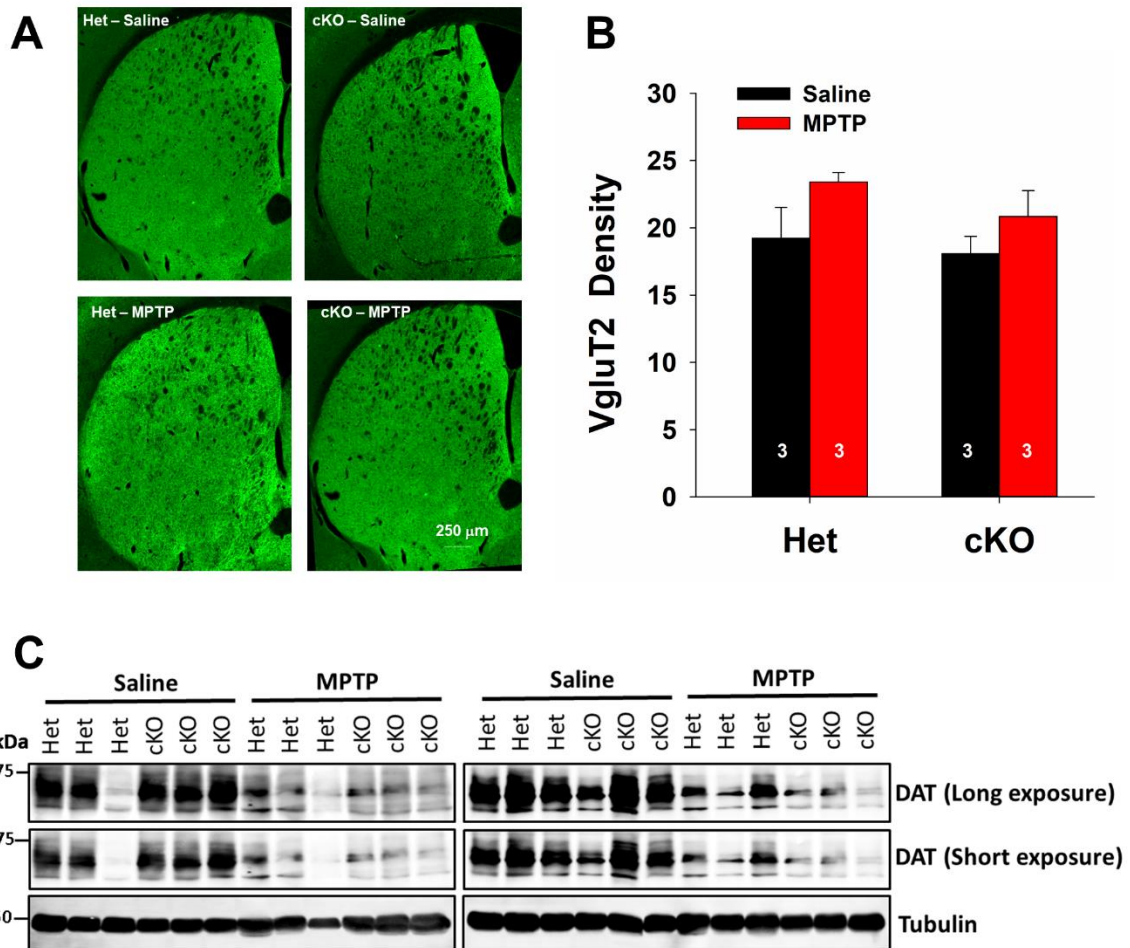
Figure S2:



**Figure S2**, Related to Fig. 1, Fig. S1: Identification of VgluT2 expression in midbrain DA neurons as assessed by VgluT2-DAT co-localization. (**A**, **B**) Representative confocal images, illustrating VgluT2 mRNA (green)- and DAT mRNA (red)-staining in the SNc and VTA in Het mice. (**C**) The mean cell counts of total DAT<sup>+</sup>, DAT<sup>+</sup> only, and DAT<sup>+</sup>-VgluT2<sup>+</sup> neurons in Het and cKO mice. VgluT2<sup>+</sup>-DAT<sup>+</sup> cell counts in cKO mice are significantly lower than those in Het mice (right panel, SNc,  $t=5.44$ ,  $p<0.01$ ; VTA,  $t=3.69$ ,  $p<0.01$ ). (**D**) The cKO mice displayed a significant reduction in percentage of DAT<sup>+</sup>-VgluT2<sup>+</sup> neurons over total DAT<sup>+</sup> neurons (SNc,  $t=5.63$ ,  $p<0.01$ ; VTA,  $t=4.56$ ,  $p<0.01$ ). \*\* $p<0.01$ , \*\*\* $p<0.001$ , compared to Het control mice. Data indicate mean  $\pm$  SEM.

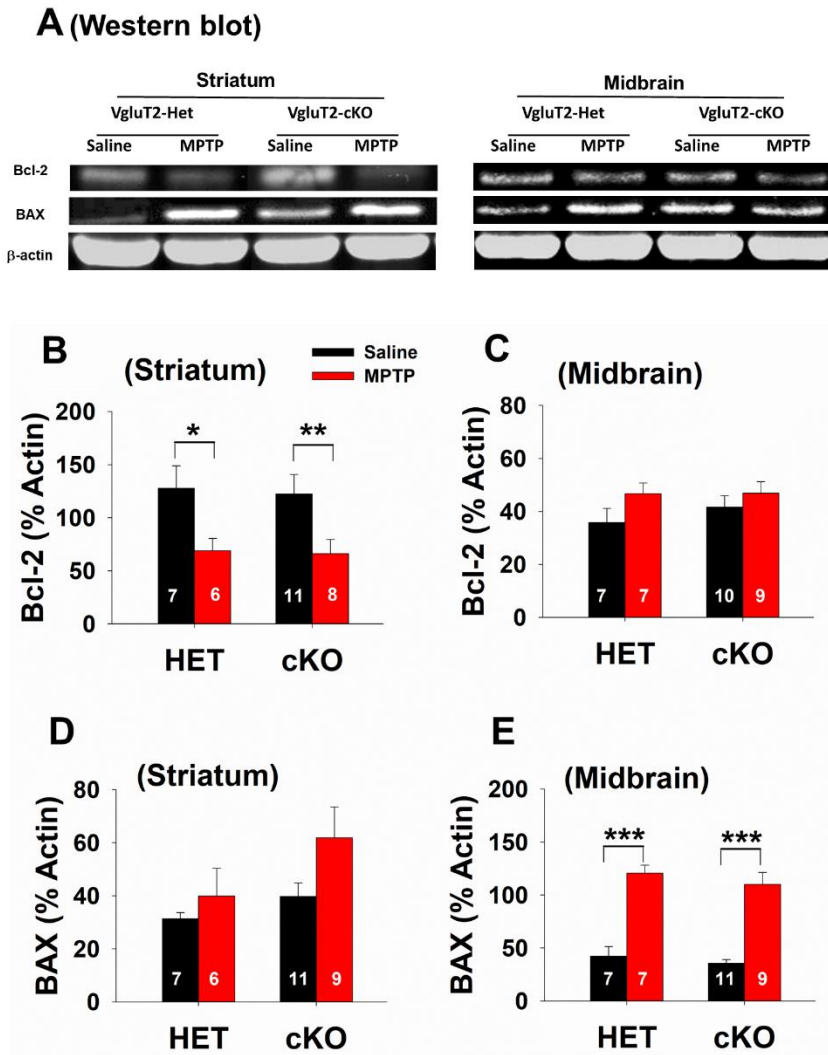


**Figure S3:**



**Figure S3**, Related to Fig. 2: VgluT2-immunostaining in the striatum and the original DAT Western blots. (**A**, **B**): Selective deletion of VgluT2 in DA neurons did not significantly alter the density of VgluT2-immunostaining in the striatum (**B**: two-way ANOVA, treatment,  $F_{1,8}=4.399$ ,  $p>0.05$ ; phenotype,  $F_{1,8}=1.26$ ,  $p>0.05$ ; treatment  $\times$  phenotype interaction,  $F_{1,8}=0.18$ ,  $p>0.05$ ). (**C**): The original Western blots (the same gels) with two different exposure times.

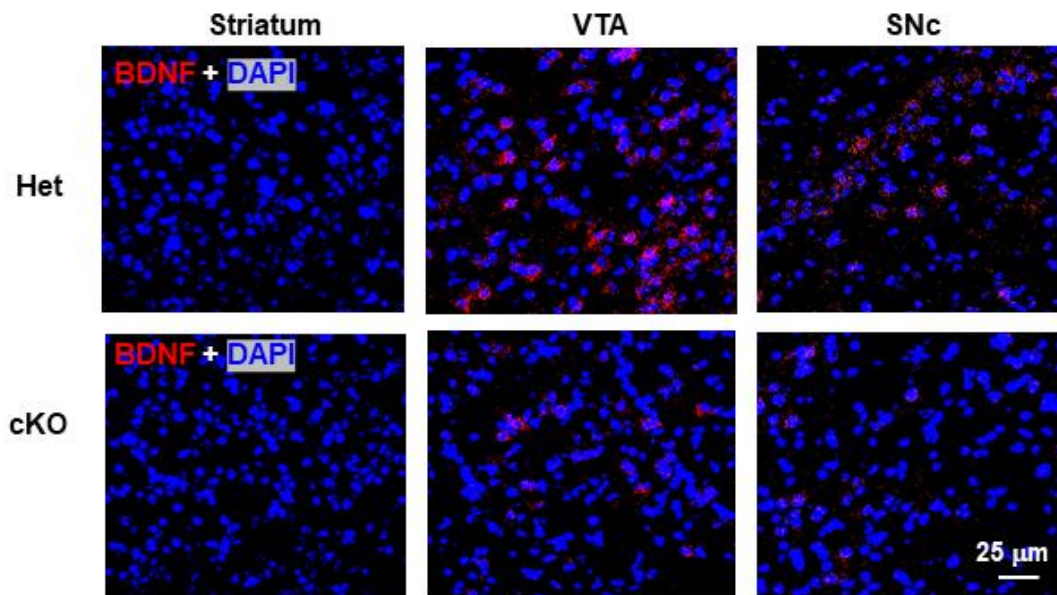
Figure S4:



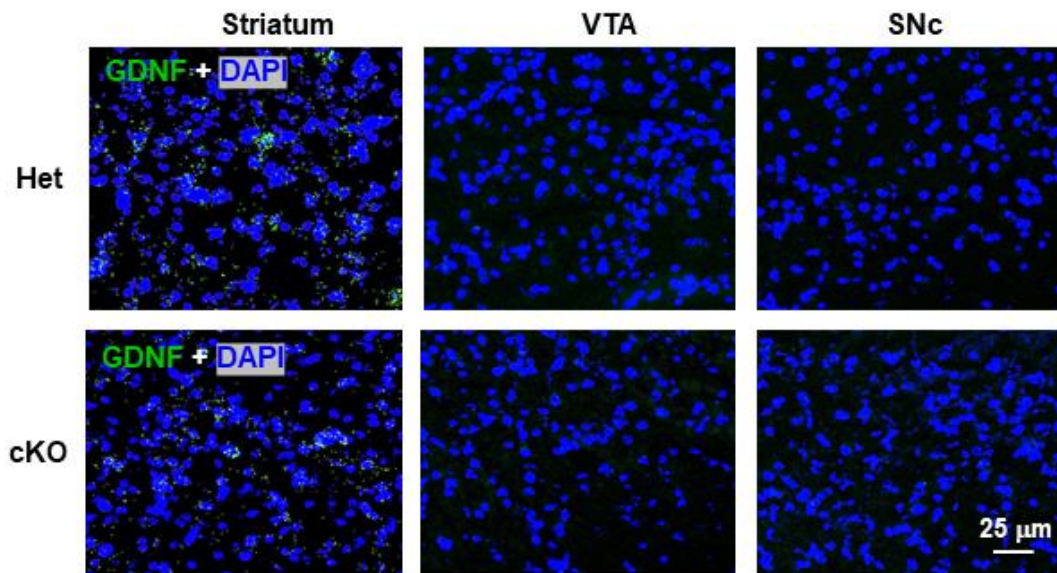
**Figure S4**, related to Figure 3. Effects of MPTP on the production of pro-apoptotic and anti-apoptotic factors in the striatum and midbrain. **(A)** Representative Western-blot assay results, indicating MPTP-induced changes in Bcl-2 and BAX in both the striatum and midbrain. **(B, C)** Mean densities of Bcl-2 bands, illustrating that MPTP pretreatment significantly decreased Bcl-2 levels in the striatum (two-way ANOVA, treatment,  $F_{1,28}=13.47$ ,  $p<0.001$ ; phenotype,  $F_{1,28}=0.26$ ,  $p>0.05$ ; treatment  $\times$  phenotype interaction,  $F_{1,28}=0.04$ ,  $p>0.05$ ), but not in the midbrain (treatment,  $F_{1,30}=3.15$ ,  $p>0.05$ ; phenotype,  $F_{1,30}=0.43$ ,  $p>0.05$ ; treatment  $\times$  phenotype interaction,  $F_{1,30}=0.39$ ,  $p>0.05$ ), in both genotypes of mice. **(D, E)** Mean densities of BAX bands, illustrating that MPTP pretreatment significantly increased BAX levels in the midbrain (treatment,  $F_{1,30}=89.15$ ,  $p<0.001$ ; phenotype,  $F_{1,30}=1.11$ ,  $p>0.05$ ; treatment  $\times$  phenotype interaction,  $F_{1,29}=0.06$ ,  $p>0.05$ ), but not in the striatum (treatment,  $F_{1,29}=3.56$ ,  $p>0.05$ ; phenotype,  $F_{1,29}=3.69$ ,  $p>0.05$ ; treatment  $\times$  phenotype interaction,  $F_{1,29}=0.70$ ,  $p>0.05$ ), in both genotypes of mice. No significant difference was found between Het and cKO mice. \* $p<0.05$ , \*\* $p<0.01$ , \*\*\* $p<0.001$ , compared to saline group of mice.

Figure S5:

**A (BDNF mRNA)**



**B (GDNF mRNA)**



**Figure S5**, related to Figure 4. BDNF and GDNF gene expression in the striatum, SNc and VTA. **(A)** RNAscope *in situ* hybridization results, illustrating that high densities of BDNF mRNA were detected in the VTA and SNc neurons, but not in the striatum. **(B)** RNAscope *in situ* hybridization results, illustrating that GDNF mRNA was detected in the striatum, not in the VTA or SNc. Notably, a significant reduction in BDNF expression in both the VTA and SNc was found in cKO mice compared to Het control mice



Figure S6:

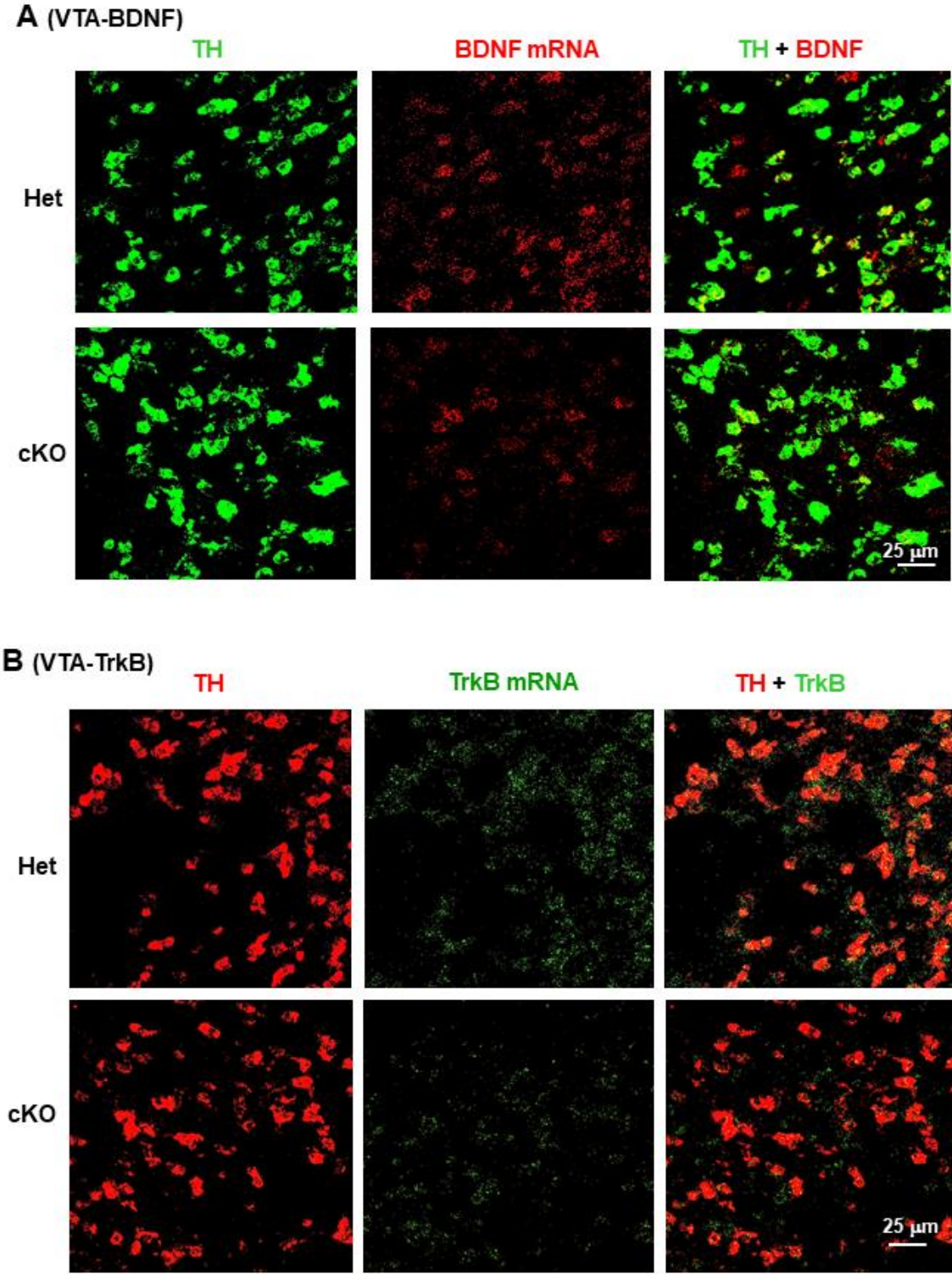


**Figure S6**, Related to Fig. 4: Representative RNAscope images, illustrating that selective deletion of VgluT2 in DA neurons in VgluT2-cKO mice significantly decreased BDNF (A) and TrkB (B) expression in VTA DA neurons.

Figure S7:

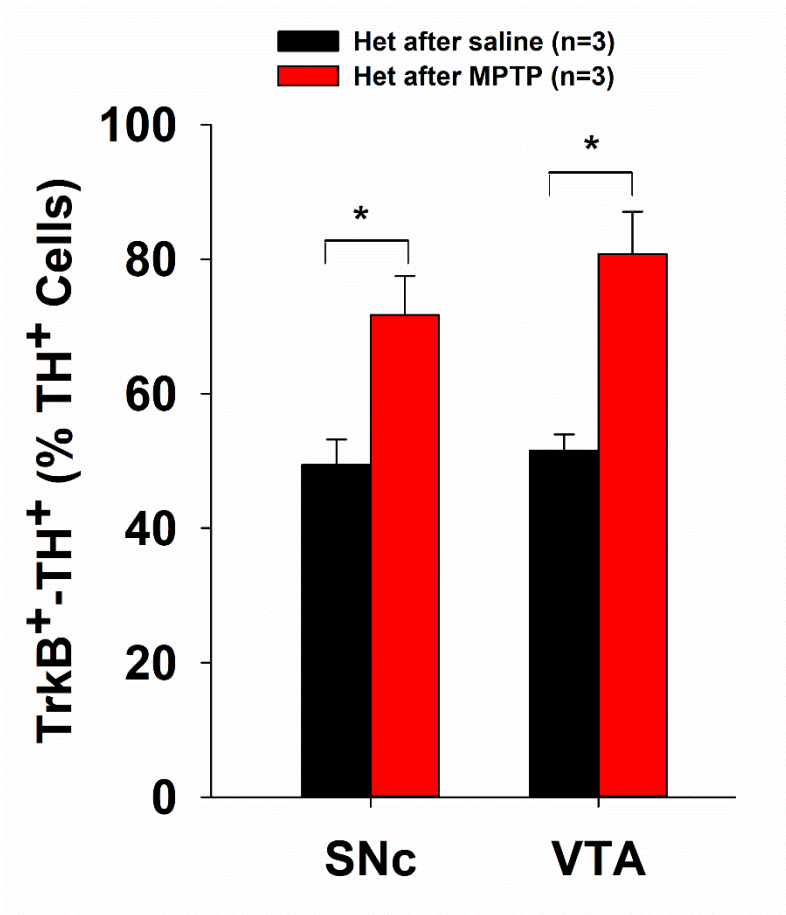
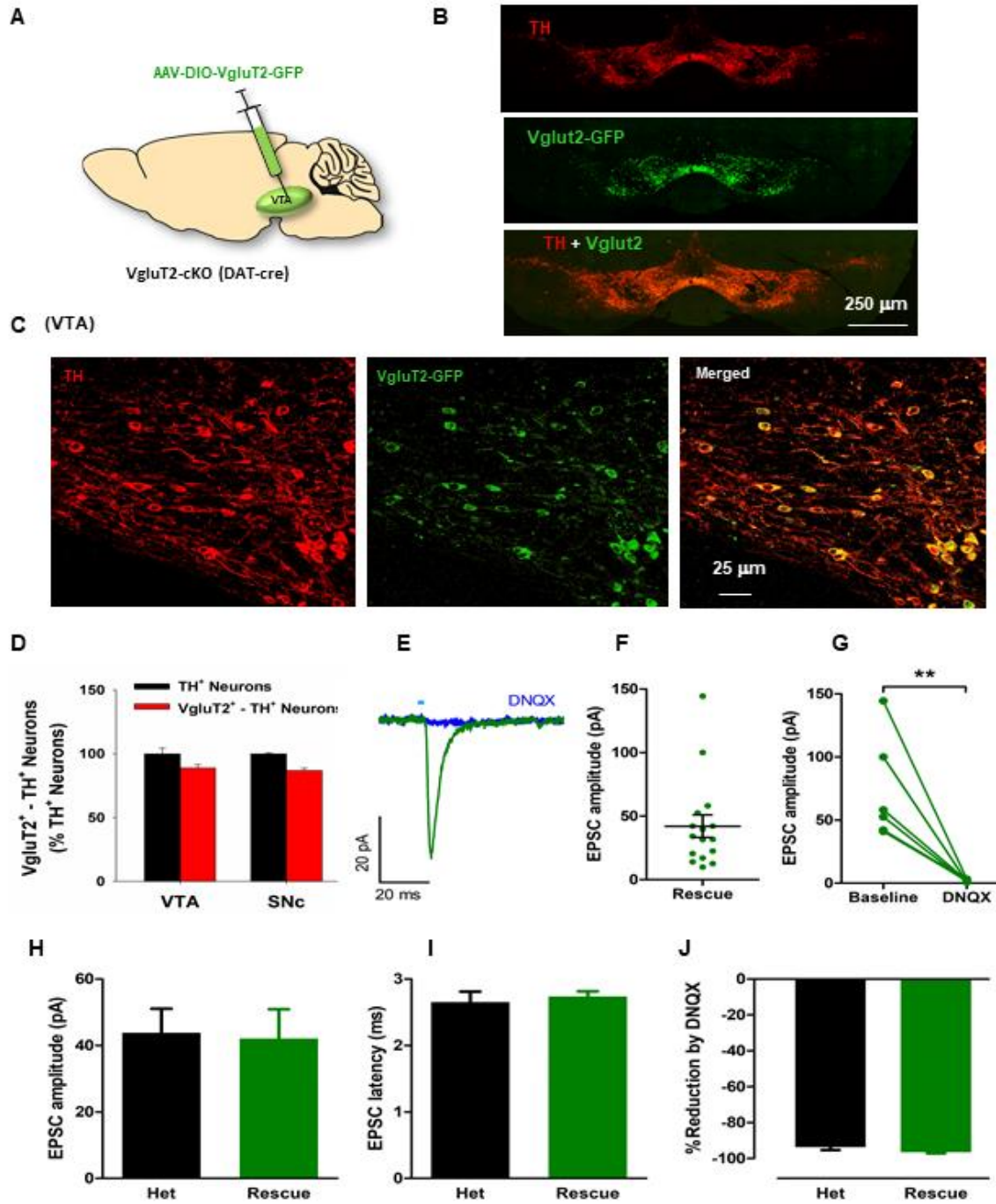


Figure S7, Related to Fig. 2, Fig. 4. TrkB mRNA staining in surviving DA neurons, illustrating higher percentages of TrkB-TH DA neurons in both the VTA and SNc in MPTP-treated Het mice than in saline control mice. \* $p < 0.05$ , compared to saline control mice.

**Figure S8:**



**Figure S8**, related to Fig. 6: VgluT2 overexpression in midbrain DA neurons of VgluT2-cKO mice. **(A)** Graphic diagram, illustrating how the AAV-DIO-VgluT2-GFP or AAV-DIO-GFP control viruses were microinjected bilaterally into the VTA. **(B)** TH-immunostaining and fluorescent VgluT2-GFP overexpression in VgluT2-rescued mice 4 weeks after AAV microinjections. **(C)** Representative confocal images, illustrating that fluorescent VgluT2-GFP is expressed in the majority of TH<sup>+</sup> DA neurons in the VTA. **(D)** Mean cell counts illustrating that ~90% TH<sup>+</sup> DA neurons expressed VgluT2 in VgluT2-cKO mice. **(E)** Representative traces showing optically-evoked post-synaptic currents (EPSCs), in the absence or presence of 10  $\mu$ M DNQX, recorded in NAc medium-spiny neurons of VgluT2-rescued mice. **(F)** Mean amplitude of optically-evoked EPSCs in VgluT2-rescued mice (16 cells from 3 mice). **(G)** Mean EPSC amplitudes in the presence or absence of DNQX in VgluT2-rescued mice. **(H)** Comparison of optically-evoked EPSC amplitudes between VgluT2-Het and VgluT2-rescued mice (6 cells, 3 mice each phenotype). **(I)** Comparison of the latency from laser onset to current onset between VgluT2-Het and VgluT2-rescued groups. **(J)** Comparison of the effectiveness of DNQX on optically-evoked EPSCs in VgluT2-Het and VgluT2-rescued mice.

## References

1. Kamens HM & Crabbe JC (2007) The parallel rod floor test: a measure of ataxia in mice. *Nat Protoc* 2:277-281.
2. McDevitt RA, *et al.* (2014) Serotonergic versus nonserotonergic dorsal raphe projection neurons: differential participation in reward circuitry. *Cell Rep* 8:1857-1869.
3. Hnasko TS, *et al.* (2010) Vesicular glutamate transport promotes dopamine storage and glutamate corelease in vivo. *Neuron* 65:643-656.
4. Qi J, *et al.* (2016) VTA glutamatergic inputs to nucleus accumbens drive aversion by acting on GABAergic interneurons. *Nat Neurosci* 19:725-733.
5. Kreitzer AC (2009) Physiology and pharmacology of striatal neurons. *Annu Rev Neurosci* 32:127- 147.
6. Song R, *et al.* (2012) Increased vulnerability to cocaine in mice lacking dopamine D3 receptors. *Proc Natl Acad Sci U S A* 109:17675-17680.
7. Tsao LI, Hayashi T, Su TP (2000). Blockade of dopamine transporter and tyrosine hydroxylase activity loss by [D-Ala(2), D-Leu(5)]enkephalin in methamphetamine-treated CD-1 mice. *Eur J Pharmacol.* 404:89-93.